Nano Today 36 (2021) 101010

Contents lists available at ScienceDirect

Nano Today

journal homepage: www.elsevier.com/locate/nanotoday

Nanosafety evaluation through feces: A comparison between selenium nanoparticles and selenite in rats

Xiaoying Lin[a,b,**], Liming Wang[b,c], Jiating Zhao[b,c], Lina He[b], Liwei Cui[c], Yuxi Gao[b,c], Chunying Chen[c,d], Yuqin Fan[e], Bai Li[b], Yu-Feng Li[b,c,*]

[a] Jilin Medical University, Jilin, 132013, Jilin, China
[b] CAS Key Laboratory for Biomedical Effects of Nanomaterials and Nanosafety, CAS-HKU Joint Laboratory of Metallomics on Health and Environment, Beijing Metallomics Facility, National Consortium for Excellence in Metallomics, Institute of High Energy Physics, Chinese Academy of Sciences, Beijing 100049, China
[c] University of Chinese Academy of Sciences, Beijing 100049, China
[d] CAS Key Laboratory for Biomedical Effects of Nanomaterials and Nanosafety, & CAS Center for Excellence in Nanoscience, & Beijing Metallomics Facility, National Centre for Nanoscience and Technology, Beijing 100191, China
[e] Shandong Provincial Maternal & Child Health Care Hospital, Cheeloo College of Medicine, Shandong University, Jinan 250014, Shandong, China

ARTICLE INFO

Article history:
Received 20 August 2020
Received in revised form 4 October 2020
Accepted 12 October 2020
Available online 1 November 2020

Keywords:
Se^0NPs
Feces
Intestinal microbiota
Metabolites
Metallomics

ABSTRACT

Nanosafety evaluation is necessary not only for nanomaterials research and development but also as a cornerstone for legal regulation. In this study, we proposed a non-invasive protocol for nanosafety evaluation through feces using metagenomics and metabolomics together with metallomics. Male SD rats were orally exposed to equal amounts of Se (Se^0NPs, 3.14 or Na_2SeO_3, 6.28 μg/kg bw) and were sacrificed after 24 h. 16S rRNA analysis and LC–MS were used to study the impact of different forms of Se on intestinal microbiota and metabolites in fecal samples. ICP-MS and synchrotron radiation X-ray fluorescence (SR-XRF) and X-ray absorption spectroscopy (XAS) were used to study the concentration and transformation of Se in gastrointestinal track and feces. It was found that Se^0NPs brought less alternation to the composition of intestinal microbiota and metabolites related to inflammation, immunity and gut-brain axis related responses than Na_2SeO_3 did. Besides, the absorbed Se^0NPs could be more efficiently converted to organic Se which explained the comparable bioavailability to Na_2SeO_3. In all, the proposed protocol combined with metagenomics, metabolomics and metallomics in this study can be used for nanosafety evaluation in a non-invasive manner and this may also be used for the screening of the nanosafety of other nanomaterials.

Introduction

Nanomaterials show unique physical and chemical properties, which have been widely used in electronics, engineering, optics, environmental remediation and medical systems, etc [1,2]. On the other hand, safety concerns are also raised about their potential adverse effects and a new discipline regarding the safety of nanomaterials, i.e. nanotoxicology is formed [3]. Nanosafety evaluation is necessary not only for nanoscience research and development but also as a cornerstone for legal regulation [1]. Cellular, tissue models as well as chemoinformatics like adverse outcome pathways can be used for nanosafety evaluation but animal models are generally required to prove these *in vitro* results [4]. Nanosafety evaluation using animal models usually requires the sacrifice of animals. Non-invasive methods for nanosafety evaluation in animal models without sacrificing animals are always desired.

Selenium (Se) is an essential trace element for animals and human beings [5,6]. However, high dose of Se are also toxic [7]. The toxicity of Se depends its chemical form: organic Se such as selenomethionine (SeMet) is less toxic than inorganic Se such as selenide (Se^{2-}), selenite (SeO_3^{2-}) and selenate (SeO_4^{2-}) [50]. The nano-sized elemental Se (Se^0NPs) are even less toxic than other inorganic Se [8]. For example, the median lethal dose (LD50) of Se^0NPs (113.0 mg/kg bw) in mice is seven times lower than that of selenite (15.7 mg/kg bw), and four times lower than that of SeMet

* Corresponding authors at: CAS Key Laboratory for Biomedical Effects of Nanomaterials and Nanosafety, CAS-HKU Joint Laboratory of Metallomics on Health and Environment, Beijing Metallomics Facility, National Consortium for Excellence in Metallomics, Institute of High Energy Physics, Chinese Academy of Sciences, Beijing 100049, China.
** Corresponding author at: Jilin Medical University, Jilin, 132013, Jilin, China.
E-mail addresses: linxy@ihep.ac.cn (X. Lin), liyf@ihep.ac.cn (Y.-F. Li).

https://doi.org/10.1016/j.nantod.2020.101010
1748-0132/

(25.6 mg/kg bw) [9]. This has also been found in other animals, such as rats [10], chickens [11,12] and goats [10,13]. More importantly, comparable bioavailability of Se^0NPs in rats with selenite was found as indicated through Se-dependent enzymes [8]. Due to its low toxicity and comparable bioavailability, Se^0NPs have been used in the treatment of many diseases, such as cancers [14] and Huntington's disease [15].

The gastrointestinal system is the first physiological barrier to the circulation of blood, which includes mechanical barriers (made up of tight junctions between epithelial cells), chemical barriers (stomach acid, bile, digestive enzymes, lysozyme, etc.), biological barriers (microecosystems), and immune barriers (gut-associated lymphoid tissue and associated immunoglobulins) [16]. In recent years, more and more attention has been paid to intestinal microbiota, which play an important role in immune and cognitive development, metabolic processes and so on. It has been found that microbiota, such as sulfur-removing *Monospora* and *Vibrio desulfidum*, are directly involved in the oxidation, reduction and methylation of Se. Therefore, the interaction of Se with the intestinal flora may contribute to its toxicity. In addition, the gut flora produces half of the body's dopamine (DA) [17], as well as many neurotransmitters, such as GABA [18] and short-chain fatty acid [19], so it is also interesting to study the metabolites of Se after oral administration.

The distinct difference in toxicity between Se^0NPs and other forms of Se made it an ideal candidate for nanosfety evaluation. Understanding the low toxicity with comparable bioavailability of Se^0NPs may shed light on finding ways for nanosafety evaluation. In this study, a non-invasive protocol for nanosafety evaluation through feces using metagenomics and metabolomics together with metallomics was proposed using Se^0NPs and Na_2SeO_3 as model compounds. Firstly, the changes of intestinal microbial community structure and metabolic products were studied using 16S rRNA and LC–MS; Secondly, the pathological morphology of intestinal tract (including large intestine and small intestine) and ADME were analyzed with ICP-MS, SR-XRF and XAS. Through these efforts, a non-invasive protocol using fecal samples as the testing matrix for nanosafety evaluation was developed.

Experimental

Animals and Se exposure

To rule out the sex difference, only male SD rats were used in this study, which were purchased from Beijing Keyu Animal Breeding Center (weight 200 ± 20 g, 4 weeks old, certificate No.: SCXK-2012-0004). A total of 15 male rats were raised in 15 metabolic cages (1 rat/cage) with 12:12 h light-dark cycle. The room temperature was 20–23°C with humidity of 40–70 %. The rats were given a standard diet and tap water *ad libitum*. The rats were randomly divided into 3 groups, ie, Na_2SeO_3, Se^0NPs and the control group with 5 rats in each group. Rats were allowed to acclimatize for one week before the start of the experiment. Then, the rats in the Se^0NPs and the Na_2SeO_3 groups were gavaged with Se^0NPs (39.2 ± 19.2 nm [20], which was kindly provided by Prof. Xueyun Gao at Institute of High Energy Physics, CAS, see supplementary materials Fig S1 for its characterization) and Na_2SeO_3 (Beijing Zhonglian Chemicals) of equal molar Se at 3.14 and 6.28 μg/kg bw, respectively dissolve in normal saline, which are much lower than their LD50. The rats in the control group were given normal saline of the same volume. After 24 h, rats were euthanized with 1% chloral hydrate and then necropsied. The brains, kidneys, livers, stomach, small and large intestines, gastrointestinal contents and fresh fecal samples were collected and kept in -80°Cbefore further analysis. All procedures used in this experiment and animal care were conducted following the rules of the Animal Ethics Committee of Institute of High Energy Physics, CAS. All applicable institutional and/or national guidelines for the care and use of animals were also followed.

16S rRNA analysis in fecal samples

Microbial DNA in fecal samples were isolated and quantified using a Qubit3.0 DNA Isolation Kit (Life Q10212) according to the manufacturer's instructions. The integrity and the size of the DNA were checked by 1% (w/v) agarose gel electrophoresis. All DNA samples were stored at −20 °C until further processing. Bacterial 16S rDNA amplification and library construction were performed according to the 16S Metagenomic Sequencing Library Preparation guide from Illumina (Forest City, CA) with minor modifications. Briefly, 2 μL of total DNA was amplified using primers targeting the 16S V3 and V4 regions (Illumina) [21]. 341F: CCCTACACGACGCTCTTCCGATCTG(barcode) CCTACGGGNGGCWGCAG-805-R:GACTGGAGTTCCTTGGCACCCGAGAATTCCA GACTACHVGGGTATCTAATCC. Pooled V3-V4 amplicon libraries were sequenced using the Illumina MiSeq platform with a V3 reagent kit. For the PCR products amplified by bacteria and archaea and the PCR products whose normal amplified fragments are above 400 bp, 0.6 times magnetic beads (Agencourt AMPure XP) are used for treatment. For fungal PCR products and other PCR products with amplified fragments less than 400 bp, magnetic beads treatment of 0.8 times is used. The Qubit2.0 DNA detection kit was used to accurately quantify the recovered DNA, so as to facilitate sequencing according to 1:1 equal mixing. When mixing in equal amounts, take 10 ng of DNA per sample, and the final sequencing concentration on the machine is 20 pmol. We used AMPure XP beads to purify the free primers and primer dimer species in the amplicon product. Samples were delivered to Sangon BioTech (Shanghai, China) for library construction using universal Illumina adaptor and index. Before sequencing, the DNA concentration of each PCR product was determined using a Qubit® 2.0 Green double-stranded DNA assay and it was quality controlled using a bioanalyzer (Agilent 2100, USA). The amplicons from each reaction mixture were pooled in equimolar ratios based on their concentration. Sequencing was performed using the Illumina MiSeq system (Illumina MiSeq, USA), according to the manufacturer's instructions (Please see S2.2 in the supplementary materials for more details).

Metabolomics profiling in fecal samples

The fresh fecal samples (100 mg) were vortex mixed with 1 mL of precooled methanol/acetonitrile (Merck, 1499230-935)/aqueous solution (2:2:1,v/v), and were ultrasonicated at low temperature for 30 min. After stored at -20°C for 10 min, the mixture were centrifuged for 20 min at 4°C at 14,000 *g* (Eppendorf 5430R), and the supernatant were taken. After vacuum drying, the supernatant were added with 100 mL acetonitrile solution (acetonitrile: water = 1:1,v/v), then centrifuged at 4°C for 15 min. The samples were then analyzed using ultra-high liquid chromatography-Q-TOF MS (HILIC UHPLC-Q-TOF MS, AB, SCIEX) [22,23]. R XCMS software was used to convert the mzXML raw data file format, in the original data. The comparison among metabolites in different groups was obtained by PCA, PLS-DA and OPLS-DA. The metabolites with $p < 0.05$ were considered as the significant differential metabolites, and were clustered with KEGG metabolic pathway analysis.

Histopathological examination in rats' gastrointestinal track

The stomach, small and large intestines were fixed with 4% formalin, then embedded in paraffin, sectioned at 4 μm and stained by hematoxylin and eosin (Besso, 719091). The histopathological

changes were evaluated by a board-certified veterinary pathologist blinded to the sample identity.

Determination of Se in tissues and fecal samples

About 200 mg freeze-dried samples were weighed into a glass digestion bottle with 3 mL HNO_3 (BV-III) and 1 mL H_2O_2 (MOS), and predigested at room temperature overnight. Then the glass digestion bottles were put on the electric heating plate for 1 h at 150°C. After digestion, it was heated at 120°C to remove residual acid until the left solution in the digestion bottles was about 1 mL, which were then diluted with 2 % HNO_3 to 4 mL. The levels of Se was determined by ICP-MS (Thermo Elemental X7, USA) [24]. A collision cell technology (CCT) was employed to avoid the $^{40}Ar^{40}Ar$ interference. Indium (SpexCertiprep Corp. USA, 10 mg/L) was used as the internal standard. The calibrating standards were prepared by diluting the Se standard stock solution (100 mg/L, Quality Control Standard 21, SpexCertiprep Co. USA) with 2 % HNO_3. A certified reference, bovine liver CRM (1577a, NBS, USA) with a certified Se value of 0.56 ± 0.07 mg/g was used with the Se recovery in the range of 90 %–110 %.

The distribution and chemical forms of Se in small intestine

The mid-ileum of the small intestine was embedded into an embedding agent (Sakura Tissue-Tek OCT, Japan), frozen at −80 °C, and then cut into 30 μm slices with a freezing microtome (Reichert-Jung, Germany). The slices were put on the Mylar membrane (polycarbonate membrane), which were stored at −20 °C before analysis. The distribution of Se was studied at BL15U1 beamline at Shanghai Synchrotron Radiation Facility (SSRF) [25]. Fluorescence data were collected using a 7-element Si (Li) detector. The beam size was 5 × 5 μm^2 and the step size at both horizontal and vertical directions was 50 μm. After normalization of the experimental data with the beam intensity (I_0), IGOR Pro was used to draw the two-dimensional distribution of Se.

The Se K-edge XANES was also recorded at BL15U1 beamline at SSRF. Na_2SeO_3, Na_2SeO_4 (Alfa Aesar), selenocystine (SeCys, Sigma), selenomethionine (SeMet, Sigma) and methylselenocystine (SeMeCys, Sigma) were used as reference materials. The XANES spectra were analyzed by WinXAS. The least square method was used for linear fitting of the XANES spectra of the samples to obtain the corresponding proportion of Se in the samples [26,27].

Statistical analysis

The statistical tests of Se concentration were performed using the software Origin 9.0, and $p < 0.05$ was considered to be significant. *t*-Test was used to compare groups with control, or among groups comparison, and then were corrected by bonferroni analysis. All data were presented as mean ± standard deviation. The detailed statistical analysis of microbial and metabolites data was listed in corresponding sections.

Results

Perturbance to intestinal microbiota by Se^0NPs or Na_2SeO_3

It was found that 24 h after exposure with equal moles of Se^0NPs and Na_2SeO_3, rats in the Na_2SeO_3 group had erected hairs with about 10 g of weight loss compared to the control group while rats in the Se^0NPs group performed normally.

The changes of intestinal microbiota are shown in Fig. 1. Using the Wayne diagram to count the number of common and unique OTUs in the sample, it was showed that the composition of the number of OTUs in samples was similar, i.e. Se^0NPs had 1068 OTUs and Na_2SeO_3 had 1186 OTUs. Fig. 1A shows that Se^0NPs was comparable to Na_2SeO_3, but was different from the control group.

The sample clustering tree diagram reflects the similarity between multiple samples through the branch structure. The length of the branches represents the distance between the samples. The more similar samples will be closer, and the branches of the same color are from the same group. As can be seen in Fig. 1B, distinct difference among the three groups was found.

RDP classifer and Blast performed species classification analysis on the obtained OTU. According to the results of taxonomy, the community composition and relative abundance of the samples on each layer (phylum, class, order, family, genus, and species) were counted. The results at the phylum and family levels are shown in Fig. 1C/D.

Fig. 1C shows the difference of ratio abundance of intestinal microbiota at the phylum level (relative abundance of > 0.05 %) in Se^0NPs, Na_2SeO_3 and control group. Fig. 1D shows the fold changes of the intestinal flora at the family level (Se^0NPs and Na_2SeO_3 group vs control group, fold change > 2 times was considered to be significantly different, relative abundance > 0.01 %).

Alterations of metabolites by Se^0NPs or Na_2SeO_3

Fig. 2A/B shows the univariate statistical analysis of metabolites in feces in the Se^0NPs, Na_2SeO_3 and the control group. In the Se^0NPs group, 192 metabolites were up-regulated and 166 down-regulated ($p < 0.05$), while in the Na_2SeO_3 group, 292 metabolites were up-regulated and 259 metabolites were down-regulated ($p < 0.05$). It showed that Se^0NPs induce less number of changed metabolites than Na_2SeO_3. Further, qualitative and quantitative analysis of the types and abundance of metabolites were studied as seen in supplementary materials. The hierarchical clustering of significantly altered metabolites in different group were compared with KEGG database [28], as shown in Fig. 5D.

Pathological damage by Se^0NPs or Na_2SeO_3 to gastrointestinal track

The pathological changes in stomach, small intestine (duodenum) and large intestine (colon) in rats treated with Se^0NPs or Na_2SeO_3 are shown in Fig. 3. Compared with Se^0NPs, Na_2SeO_3 caused severe destruction of the fundus gland structure of the stomach. In addition, a large number of inflammatory cell clusters in the lamina propria of the duodenal submucosa, intestinal villi become latent, etc. were found, destroyed the secretion-related cups inside stellate cells, M immune cells and colonic mucosal epithelial cells necrosis, goblet cells, crypts, etc in the Na_2SeO_3 group.

Accumulation of Se in gastrointestinal track after exposure to Se^0NPs or Na_2SeO_3

The accumulation of Se in gastrointestinal system was much higher than organs (Se concentration in liver was only over 40 ng/g in Na_2SeO_3 group as shown in Figure S2), suggesting that the gastrointestinal system is the mainly target organ with oral exposure to Na_2SeO_3 or Se^0NPs by 24 h.

Se concentration in the gastrointestinal wall, gastrointestinal contents and feces of rats is shown in Fig. 4. Lower concentration of Se was found in the stomach, small and large intestinal wall in Se^0NPs group than that in Na_2SeO_3 group ($p < 0.01$). This indicates that Se^0NPs was less absorbed than Na_2SeO_3 by the gastrointestinal track or Se^0NPs may be more easily absorbed into the blood and quickly transported to other parts of the body. The Se concentration in gastrointestinal contents was higher than that in the gastrointestinal walls, suggesting that Se was not totally absorbed

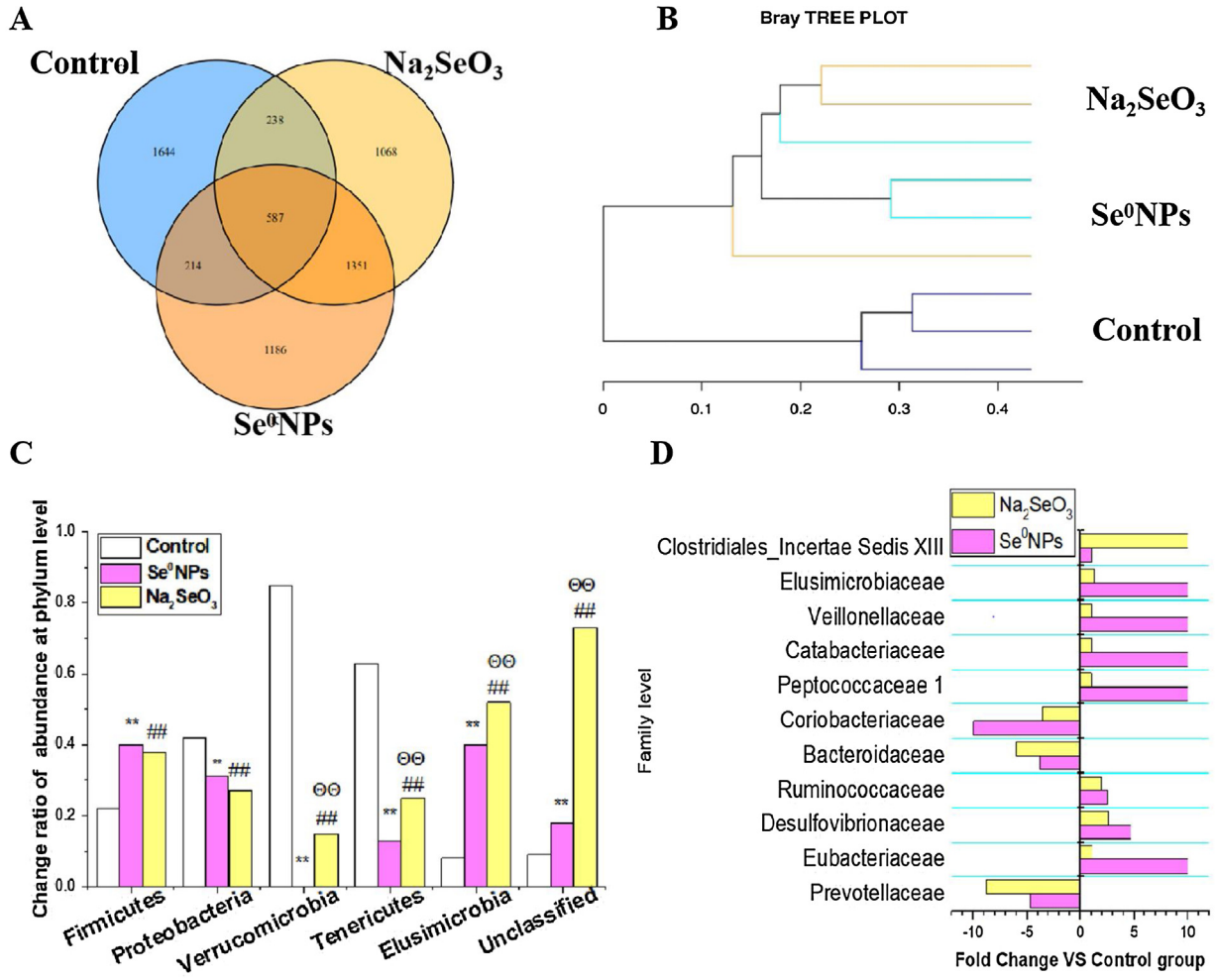

Fig. 1. The structural and functional changes of intestinal microbiota in the feces of rats through 16S rRNA sequencing. (A) OTU values; (B) Bray TREE plots; (C) Phylum-level, $^{**}p < 0.01$ Se^0NPs VS Control, $\#\#p < 0.01$, Na_2SeO_3 VS Control, $\theta\theta p < 001$ Na_2SeO_3 VS Se^0NPs; (D) Family-level (Fold change >2, $n = 3$).

in 24 h. Higher Se was found in feces when exposed to Se^0NPs than Na_2SeO_3($p < 0.01$), which suggests that Se^0NPs was less absorbed than Na_2SeO_3. This was in consistent with the results got by other researchers [29].

The spatial distribution and chemical forms of Se in small intestine wall

The duodenum is the main part for Se absorption [30]. The spatial distribution of Se in duodenum wall was studied using SR-XRF, which is shown in Fig. 5. The fluorescence intensity has been normalized, therefore, the fluorescence intensity represented the relative levels of Se. It can be seen that less Se was found in the duodenum wall in the Se^0NPs group than that in the Na_2SeO_3 group while higher levels of Se was found in the intestinal content of the Se^0NPs group (Figure 5B1 and B2). This again suggested that Se^0NPs was less absorbed by the intestinal wall than Na_2SeO_3, which is consistent with the intestinal accumulation of Se as shown in Fig. 4. In addition, it can be seen that Se in the Se^0NPs group was evenly distributed in the small intestinal wall while many of them were in the intestine mucosal layers in the Na_2SeO_3 group (Figure 5B1 and B2).

The chemical forms of Se in duodenum with high level of Se were studied using μ-XANES, as shown in Figure 5C1/C2. In the Se^0NPs group as shown in Figure 5C1, Se was may mainly in the form of Se-C (using SeCys as reference material) and Se^0, with the proportion of 58 % and 42 %, respectively through least-square fitting. Se was mainly in the form of Se-C (using SeMet as reference material) and Se^{6+} in the Na_2SeO_3 group, with the proportion of 32 % and 68 % (Figure 5C2), respectively.

Previous study found that about 20 % of Se was still in the form of Se^0 after exposure to Se^0NPs, and Se^0NPs was less absorbed than Na_2SeO_3 [29]. This may also explain the relative low toxicity of Se0NPs and its low perturbance to gut microbiota and metabolites.

Discussion

Different changes in intestinal microbes and metabolites in rats feces caused by Se^0NPs and Na_2SeO_3

Compared with the control group, Na_2SeO_3 caused the much decreased abundance of beneficial bacteria than Se^0NPs, such as *Proteobacteria* (Control 42 %, Se^0NPs 31 %, Na_2SeO_3 27 %, Fig. 1C) [31], and the increased abundance of harmful bacteria, such as *Eluaimicrobia* (Control 8%, Se^0NPs 40 %, Na_2SeO_3 52 %) [32], and the uncalssified (Control 9 %, Se^0NPs 18 %, Na_2SeO_3 73 %). Se^0NPs induced the increased abundance of beneficial bacteria, such as *Firmicutes* (Control 22 %, Se^0NPs 40 %, Na_2SeO_3 38 %) [33], *Proteobacteria* (Control 42 %, Se^0NPs 37 %, Na_2SeO_3 31 %) [33], and the decreased abundance of harmful bacteria, such as *Verrucomicrobia* (Control 85 %, Se^0NPs 0%, Na_2SeO_3 15 %) [33], and *Tenericutes* (Control 63 %, Se^0NPs 13 %, Na_2SeO_3 25 %) [33]. This indicated that

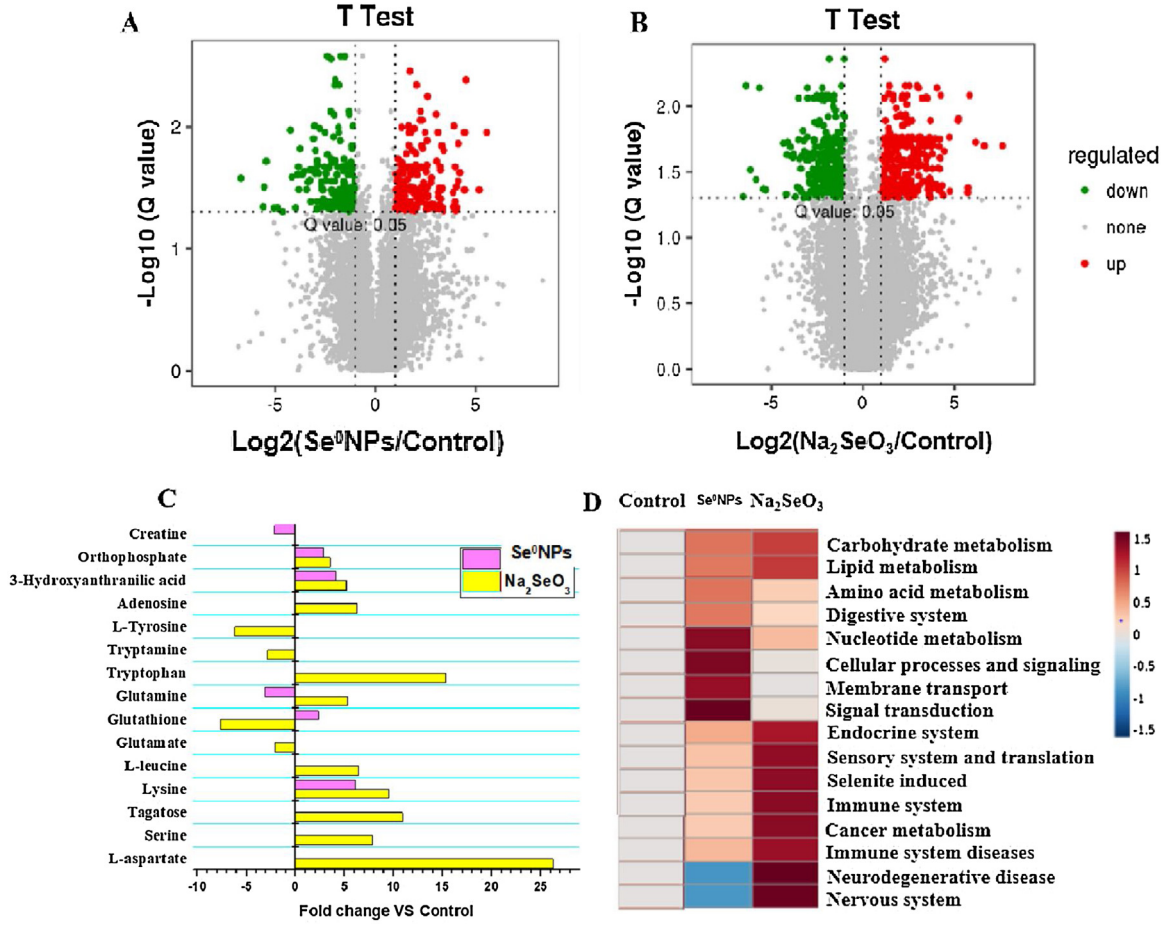

Fig. 2. Exposure of (A) Se^0NPs or (B) Na_2SeO_3 alters the metabolites in rat feces. (red and green represent up and down, with multiple changes of > 1.5, $p < 0.05$, and gray multiple changes of <1.5, $p > 0.05$); (C) Na_2SeO_3 and Se^0NPs changed certain gut-brain axis related metabolites (fold changes against the control group); (D) Differential metabolite KEGG pathway analysis induced by Se^0NPs or Na_2SeO_3 ($n = 3$).

Se^0NPs caused less toxic effects on intestinal microorganisms than Na_2SeO_3.

Fig. 1D shows that Na_2SeO_3 caused the greater increased abundance of *Clostridiales_Incertae Sedis XIII* than Se^0NPs, which has been reported to be related to the immune system [34]. This suggests that Na_2SeO_3 may disrupt the intestinal immune barrier after oral exposure to rats. In addition, Na_2SeO_3 caused the greater decreased abundance of *Prevotellaceae* and *Bacteroidaceas* than Se^0NPs, which participated the synthesis effect in short-chain fatty acids, affected the intestinal brain axis pathway and regulated the nervous system [35]. It was also found that Se^0NPs caused a decrease in the abundance of *Vibrio desulfurus*, which is an important bacterium in the Se metabolism, and plays an important role in the conversion of elemental Se to organic Se [36,37]. Besides, Se^0NPs also caused the up-regulation of *Elusimicrobiaceae*, *Veilonellaceae*, *Catabacteriaceae*, *Peptococeaceae*, and the down-regulation of the abundance of *Coriobactericeae*, *Ruminococeaceae*, *Eubactriaceae*. Whether these change of gut microbes participate in the absorption or transform of Se^0NPs is still not clear [38].

Se^0NPs and Na_2SeO_3 bring different changes in the abundance of rat gut microbes. However, the underlying mechanism for this is still not clear. One possible reason may be ascribed to the fact that the toxicity of Na_2SeO_3 is greater than that of Se^0NPs. This may causes the suppression of a large number of beneficial intestinal microbes when exposed to Na_2SeO_3 which then lead to an increase in the relative abundance of harmful bacteria. On the other hand, due to the low toxicity of Se^0NPs while Se is essential to them, it will facilitate the growth of beneficial intestinal microbes.

It was found that Na_2SeO_3 caused much more changes of metabolites relative to gut-brain axis than Se^0NPs did (Fig. 2C), such as the up-regulation of Adenosine [38], Tryptophan [39], Glutamine [40], L-Leucine [41], Lysine [42], Tagatose [43], Serine [44], L-aspartate [45], and the down-regulation of L-tyrosine [46], Tryptophan, Glutathione [47], Glutamate [48]. Se^0NPs induced the down-regulation of Creatine [49], Glutamine, and the up-regulate of Lysine. It suggested that Na_2SeO_3 induced the disorders of the nervous system while Se^0NPs did not.

Difference in metabolites related to carbohydrate metabolism, digestive system, amino acid metabolism, and lipid metabolism was also found. It showed that Na_2SeO_3 caused the changes of metabolites related to immune system, and neuro-degenerative diseases, etc. These metabolic pathways are related to the occurrence of the immunity and neurotrophic responses, while Se^0NPs induced the changes of metabolites related to the nucleotide metabolism, cellular processes and signaling, signal transduction and membrane transport. These results further showed the distinct difference between Na_2SeO_3 and Se^0NPs.

The pathological damage to the intestines, and the absorption and transformation of Se^0NPs and Na_2SeO_3 confirm the changes of gut microbiota and metabolites

From the above results, Se^0NPs brought less damage to the mucosal barrier and was less absorbed by the intestinal wall than Na_2SeO_3. This may be a reason for different toxicity between Se^0NPs and Na_2SeO_3. Further, Se is usually absorbed by firstly being con-

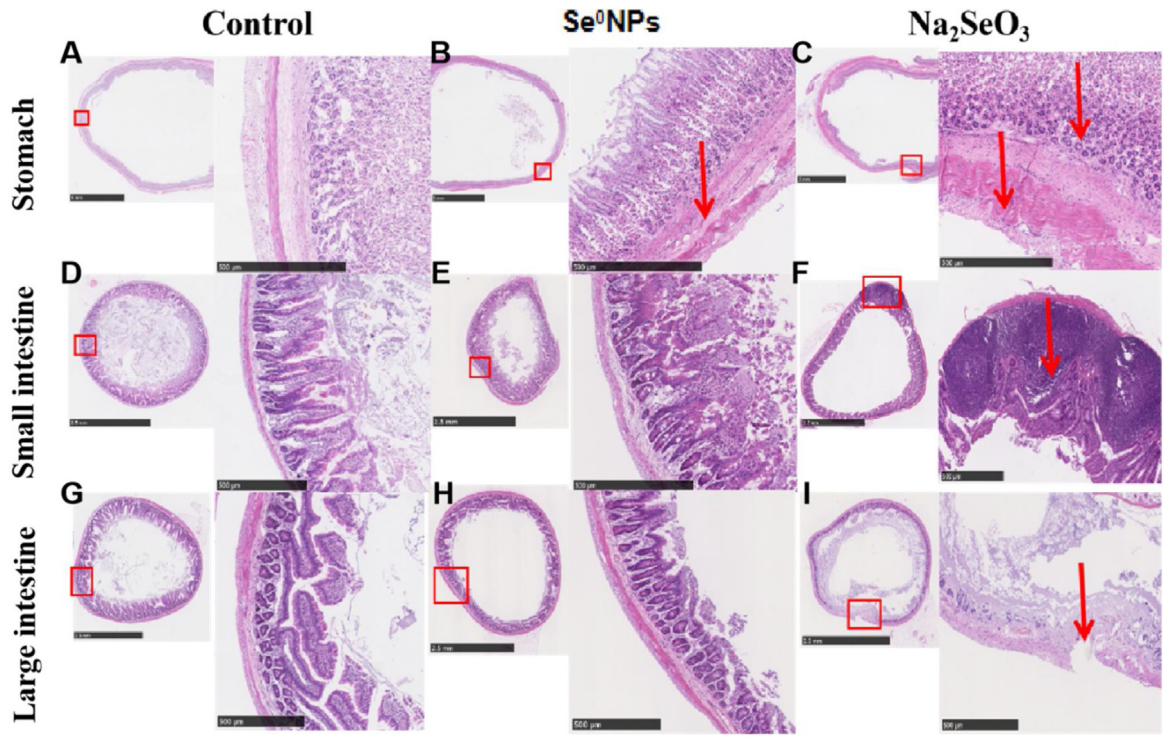

Fig. 3. Pathological changes of stomach(A-C), small intestine (ileum) (D-F) and large gut (colon)(G-I) in rats treated with Se^0NPs or Na_2SeO_3 by H&E staining (40X, left, 400X, right). The red arrows in B, C, F and I showed the pathological changes. i.e., compared with Se^0NPs, Na_2SeO_3 caused severe destruction of the fundus gland structure of the stomach(C), and induce a large number of inflammatory cell clusters in the lamina propria of the duodenal submucosa, intestinal villi become latent, etc. were found, destroyed the secretion-related cups inside stellate cells, M immune cells and colonic mucosal epithelial cells necrosis, goblet cells, crypts, etc (F, I).

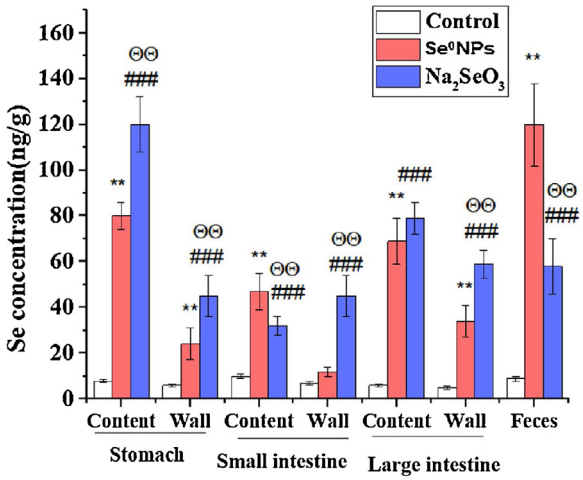

Fig. 4. Se concentration in the gastrointestinal wall, contents and feces of rats. ** p <0.01, ### p < 0.001 Se^0NPs or Na_2SeO_3 group compared with the control group; θθ p <0.01, Na_2SeO_3 group compared with Se^0NPs group (n = 5).

verted into selenides and then converted into organic selenium for biological use. Se^0NPs was more easily be transformed to organic Se like SeCys while most of the Na_2SeO_3 was oxidated to Na_2SeO_4, which is more toxic than the former [50]. This may explain although Se^0NPs was less intestinal absorbed than Na_2SeO_3 while still have comparable biavailability [51]. In addition, compared with Se^0NPs, a large number of inflammatory cell clusters in the lamina propria of the duodenal submucosa, intestinal villi became latent, destroyed the secretion-related cups inside stellate cells, M immune cells and colonic mucosal epithelial cells necrosis, goblet cells, crypts, etc in the Na_2SeO_3 group. This directly confirms its destruction of inflammatory, immune and nervous system caused by Na_2SeO_3 other than by Se^0NPs.

Conclusion

In all, through the proposed method combined with metagenomics, metabolomics and metallomics in this study as illustrated in Fig. 6, the two forms of Se could be distinctively differentiated: 1) Through 16S rRNA sequencing in feces, it was found that Na_2SeO_3 was more toxic than Se^0NPs on gut microbial barrier with a large number of bacteria involved in the reduction of Na_2SeO_3 increased; 2) Through metabolomics study on fecal samples, it was found that Na_2SeO_3 brought more disrupted metabolites related to gut-brain axis etc than by Se^0NPs; These results were further proved through 3) metallomics study, which found the absorption efficiency of Se^0NPs in the intestine was lower than Na_2SeO_3, while the absorbed Se^0NPs was more easily converted into organic Se; and 4) pathological analysis further proved that Na_2SeO_3 brought more damage to gut intestinal mucosal barrier, and triggered a lot of stomach necrosis of secretory and immune cells in the intestine. Although we have analyzed the difference between the two forms of selenium on the intestinal microbes and metabolites of rats and their transformation in the intestinal tract, it is not possible to get a definite conclusion on how and why the intestinal microbes were regulated. Further studies are necessary to explore the underlying mechanism for the distinct differences between Se^0NPs and Na_2SeO_3.

Our proposed protocol can be used for nanosafety evaluation in a non-invasive manner and this may also be used for the screening of the nanosafety of other nanomaterials.

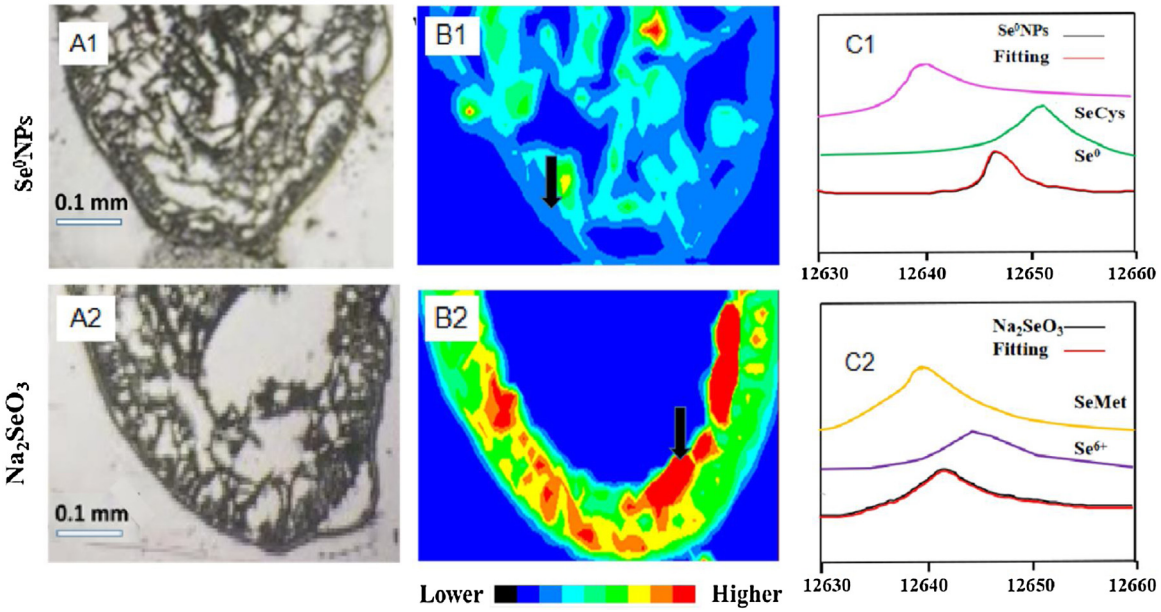

Fig. 5. The spatial distribution of Se in small intestine wall (A1/A2 bright field, 40X; B1/B2 fluorescence intensity). Se was found in the duodenum wall in the Se^0NPs group than that in the Na_2SeO_3 group while higher levels of Se was found in the intestinal content of the Se^0NPs group. The chemical forms of Se in the small intestine walls as pointed by black arrows in B1/B2 were studied by μ–XANES (C1/C2). Se was mainly in the form of SeCys and Se^0 in the Se^0NPs group while it was SeMet and Se^{6+} in the Na_2SeO_3 group.

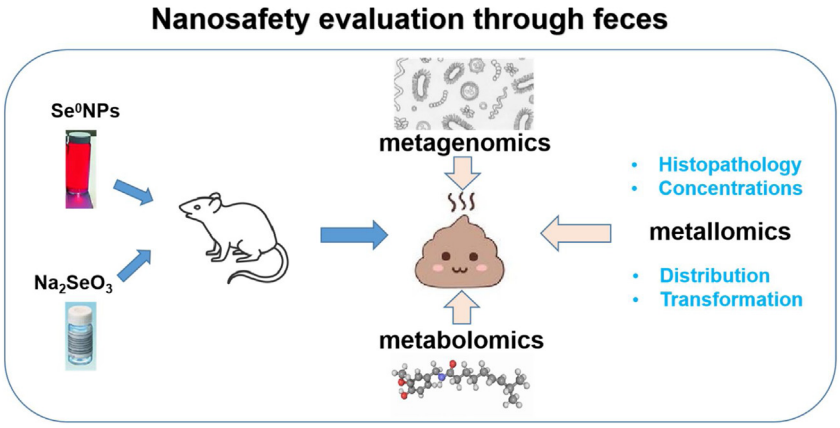

Fig. 6. The working scheme of the proposed method combined with metagenomics, metabolomics and metallomics.

CRediT authorship contribution statement

Xiaoying Lin: Data curation, Writing - original draft, Visualization, Investigation. **Liming Wang:** Data curation, Writing - original draft, Visualization, Investigation, Software, Validation. **Jiating Zhao:** Data curation, Writing - original draft, Visualization, Investigation. **Lina He:** Visualization, Investigation, Software, Validation. **Liwei Cui:** Visualization, Investigation, Software, Validation. **Yuxi Gao:** Supervision. **Chunying Chen:** Conceptualization, Methodology, Software, Supervision, Writing - review & editing. **Yuqin Fan:** Visualization, Investigation. **Yu-Feng Li:** Conceptualization, Methodology, Software, Supervision, Writing - review & editing.

Declaration of Competing Interest

All authors declare there is no copyright disputes.

Acknowledgements

The authors are grateful for the financial support from the Ministry of Science and Technology of China (2016YFA0201600), National Natural Science Foundation of China (11975247, 11475496), Guizhou Department of Science and Technology (No. QKH-2016-2804), and Jilin Medical College Doctoral Research Startup Fund Project (JYBS2019011). We gratefully acknowledged the staff from BL15U1 beamline at Shanghai Synchrotron Radiation Facility and 4W1B at Beijing Synchrotron Radiation Facility for beam time allocation and assistance during data collection.

Appendix A. Supplementary data

Supplementary material related to this article can be found, in the online version, at doi:https://doi.org/10.1016/j.nantod.2020.101010.

References

[1] G. Fang, W. Li, X. Shen, J.M. Perez-Aguilar, Y. Chong, X. Gao, Z. Chai, C. Chen, C. Ge, R. Zhou, Differential Pd-nanocrystal facets demonstrate distinct antibacterial activity against gram-positive and gram-negative bacteria, Nat. Commun. 9 (2018) 129.

[2] J. Du, Z. Gu, L. Yan, Y. Yong, X. Yi, X. Zhang, L. Liu, R. Wu, C. Ge, C. Chen, Y. Zhao, Poly(vinylpyrollidone) and selenocysteine modified Bi_2Se_3 nanoparticles enhance radiotherapy efficacy in tumor and promote radioprotection in normal tissues, Adv. Mater. 29 (2017), 1701268.

[3] Y. Zhao, H. Nalwa, Nanotoxicology: Interactions of Nanomaterials With Biological Systems, American Scientific Publishers, 2007.

[4] C. Chen, Y.-F. Li, Y. Qu, Z. Chai, Y. Zhao, Advanced nuclear analytical and related techniques for the growing challenges in nanotoxicology, Chem. Soc. Rev. 42 (21) (2013) 8266–8303.

[5] M.P. Rayman, Selenium and human health, Lancet 379 (9822) (2012) 1256–1268.

[6] C. Achilli, A. Ciana, G. Minetti, Brain, immune system and selenium: A starting point for a new diagnostic marker for Alzheimer's disease? Perspect. Public Health 138 (4) (2018) 223–236.

[7] Y. Li, J. Zhao, L. He, L. Wang, L. Cui, B. Li, Y. Li, Fast quantification and speciation of selenium in dietary supplements through handheL.d XRF and synchrotron radiation XAS, Atom. Spectr. 41 (3) (2020) 127–130.

[8] J. Zhang, Y. Gao, L. Zhang, Y. Bao, Biological effects of a nano red elemental selenium, BioFactors 15 (1) (2001) 27–38.

[9] H. Wang, J. Zhang, H. Yu, Elemental selenium at nano size possesses lower toxicity without compromising the fundamental effect on selenoenzymes: comparison with selenomethionine in mice, Free Radic. Biol. Med. 42 (10) (2007) 1524–1533.

[10] X. Jia, N. Li, J. Chen, A subchronic toxicity study of elemental nano-Se in sprague dawley rats, Life Sci. 76 (17) (2005) 1989–2003.

[11] X. Zhou, Y. Wang, Influence of dietary nano elemental selenium on growth performance, tissue selenium distritution, meat quality, and glutathione peroxidase activity in Guangxi Yellow chicken, Poult. Sci. 90 (3) (2011) 680–686.

[12] C. Hu, Y. Li, L. Xiong, H. Zhang, J. Song, M. Xia, Comparative effects of nano elemental selenium and sodium selenite on selenium retention in broiler chickens, Anim. Feed Sci. Technol. 177 (3–4) (2012) 204–210.

[13] L. Shi, W. Xun, W. Yue, C. Zhang, Y. Ren, Q. Wang, R. Yang, F. Lei, Effect of sodium selenite, Se-yeast and nano-elemental selenium on growth performance, Se concentration and antioxidant status in growing male goats, Small Rumin. Res. 96 (1) (2011) 49–52.

[14] J. Pi, J. Jiang, H. Cai, F. Yang, H. Jin, P. Yang, J. Cai, Z. Chen, GE11 peptide conjugated selenium nanoparticles for EGFR targeted oridonin delivery to achieve enhanced anticancer efficacy by inhibiting EGFR-mediated PI3K/AKT and Ras/Raf/MEK/ERK pathways, Drug Deliv. 24 (1) (2017) 1549–1564.

[15] W. Cong, R. Bai, Y.-F. Li, L. Wang, C. Chen, Selenium nanoparticles as an efficient nanomedicine for the therapy of Huntington's Disease, ACS Appl. Mater. Interfaces 11 (38) (2019) 34725–34735.

[16] X. Cui, B. Lin, X. Wang, C. Chen, The nano-intestine interaction: understanding the location-oriented effects of engineered nanomaterials in the intestine, Small 16 (21) (2020), 1907665.

[17] A. Abizaid, Z. Liu, Z.B. Andrews, M. Shanabrough, E. Borok, J.D. Elsworth, R.H. Roth, M.W. Sleeman, M.R. Picciotto, M.H. Tschöp, X. Gao, T.L. Horvath, Z. Liu, M.H. Tschöp, X. Gao, Ghrelin modulates the activity and synaptic input organization of midbrain dopamine neurons while promoting appetite, J. Clin. Invest. 116 (12) (2007) 3229–3239.

[18] M. Liu, P. Zheng, B. Zeng, M. Liu, J. Chen, J. Pan, Y. Han, Y. Liu, K. Cheng, K. Zhou, H. Wang, X. Zhou, S. Gui, W.P. Seth, M. Wong, L. Julio, H. Wei, P. Xie, The gut microbiome from patients with schizophrenia modulates the glutamine-GABA cycle and schizophenia relevant behaviors in mice, Sci. Adv. 5 (2019) 8317, http://dx.doi.org/10.1126/sciadv, eaau Aau8317.

[19] S. Charoensiddhi, M.A. Conlon, M.S. Vuaran, C.M.M. Fraco, W. Zhang, Impact of extraction processes on prebiotic potential of the brown seaweed Ecklonia radiata by in vitro human gut bacteria fermentation, J. Funct. Foods 24 (2016) 221–230.

[20] J. Zhao, X. Liang, N. Zhu, L. Wang, Y. Li, Y. Li, L. Zheng, Z. Zhang, Y. Gao, Z. Chai, Immobilization of mercury by nano-elemental selenium and the underlying mechanisms in hydroponic-cultured garlic plant, Environ. Sci. Nano 7 (2020) 1115–1125.

[21] X. Wu, H. Zhang, J. Chen, S. Shang, Q. Wei, J. Yan, X. Tu, Comparison of the fecal microbiota of dholes high-throughput Illumina sequencing of the V3-V4 region of the 16S rRNA gene, Appl. Microbiol. Biotechnol. 100 (8) (2016) 3577–3586.

[22] J. Ivanisevic, Z. Zhu, L. Plate, R. Tautenhahn, S. Chen, P. Brien, C.H. Johnson, M.A. Marletta, G.J. Patti, G. Siuzdak, Toward 'omic' scale metabolite profiling: a dual separation-mass spectrometry approach for coverage of lipid and central carbon metabolism, Anal. Chem. 85 (2013) 6876–6884.

[23] H.P. Benton, J. Ivanisevic, N.G. Mahieu, M.E. Kurczy, C.H. Johnson, L. Franco, D. Rinehart, E. Valentine, H. Gowda, B.K. Ubhi, R. Taugenhahn, A. Gieschen, M.W. Fiedlds, G.J. Patti, G. Siuzdak, Autonomous metabolomics for rapid metabolite identification in global profiling, Anal. Chem. 87 (2015) 884–891.

[24] Y.-F. Li, J. Zhao, Y.-F. Li, J. Zhang, Y.-F. Li, Y. Gao, C. Chen, M. Luo, R. Huang, J. Li, The concentration of selenium matters: a field study on mercury accumulation in rice by selenite treatment in Qingzhen, Guizhou, China, Plant Soil 392 (1–2) (2015) 195–205.

[25] L. Zhang, S. Yan, S. Jiang, K. Yang, H. Wang, S. He, D. Liang, L. Zhang, Y. He, X. Lan, C. Mao, J. Wang, H. Jiang, Y. Zheng, Z. Dong, L. Zeng, Hard X-ray micro-focusing beamline at SSRF, Nucl. Sci. Tech. 26 (6) (2015) 060101–060108.

[26] B. Deng, Q. Yang, G. Du, Y. Tong, H. Xie, T. Xiao, The progress of X-ray fluorescence computed tomography at SSRF, Nucl. Instrum. Methods Phys. Res. 305 (2013) 5–8.

[27] Y. Takata, T. Yokoyama, S. Yagi, N. Happo, H. Sato, K. Seki, T. Ohta, Y. Kitajima, H. Kuroda, Thiophenol adsorption on Ni(100) studied by S K-edge SEXAFS and XANES, Surf. Sci. Lett. 259 (1991) 266–274.

[28] K. Minoru, The KEGG database, Novartis Found. Symp. 247 (2002) 91–101.

[29] L. Katrin, H. Niels, H. Marianne, A.P. Sonia, G. Bente, H.M. Laura, M. Alicja, R.L. Henrik, H.L. Erik, Absorption, distribution, metabolism and excretion of selenium following oral administration of elemental selenium nanoparticles or selenite in rats, Metallomics 6 (2014) 330–337.

[30] R.J. Shamberger, Selenium in the environment, Sci. Total Environ. 17 (1) (1981) 59–74.

[31] R. Nadia, H. Utpal, Z. Yunzeng, M. Dewdney, N. Wang, Characterization of antimicrobial-producing beneficial bacteria isolated from huanglongbing Escape Citrus trees, Front. Microbiol. 8 (2017) 2415.

[32] E. Cabiscol, J. Tamarit, J. Ros, Oxidative stress in bacteria and protein damage by reactive oxygen species, Int. Microbiol. 3 (1) (2000) 3–8.

[33] C. Vincent, D.A. Stephens, V.G. Loo, T.J. Edens, M.A. Behr, K. Dewar, A.R. Manges, Reductions in intestinal Clostridiales precede the development of nosocomial Clostridium difficile infection, Microbiome 1 (1) (2013) 1–11.

[34] R.M. Garruto, R. Yanagihara, D.C. Gajdusek, Models of environmentally induced neurological disease: epidemiology and etiology of amyotrophic lateral sclerosis and parkinsonism-dementia in the Western Pacific, Environ. Geochem. Health 12 (1–2) (1990) 137–151.

[35] M.J. Herbel, T.M. Johnson, R.S. Oremland, T.D. Bullen, Fractionation of selenium isotopes during bacterial respiratory reduction of selenium oxyanions, Geochim. Cosmochim. Acta 64 (21) (2000) 3701–3709.

[36] B.E. Jacobson, G. Lockitch, Direct determination of selenium in serum by graphite-furnace atomic absorption spectrometry with deuterium background correction and a reduced palladium modifier: age-specific reference ranges, Clin. Chem. 34 (4) (1988) 709–714.

[37] D. Song, Z. Lu, F. Wang, Y. Wang, Biogenic nano-selenium particles effectively attenuate oxidative stress-induced intestinal epithelial barrier injury by activating the Nrf2 antioxidant pathway, J. Anim. Sci. 95 (4) (2017) 20–21.

[38] Y. Liu, J. Chen, X. Li, X. Zhou, Y. Hu, S. Chu, Y. Peng, N. Chen, Research progress on adenosine in central nervous system diseases, CNS Neurosci. Ther. 25 (9) (2019) 899–910.

[39] K. Nakamura, H. Hasegawa, Developmental role of tryptophan hydroxylase in the nervous system, Mol. Neurobiol. 35 (1) (2007) 45–53.

[40] I. Pérez-Neri, J. Ramírez-Bermúdez, C. Ojeda-López, Glutamine and citrulline concentrations reflect nitric oxide synthesis in the human nervous system, Neurologria 35 (2) (2019) 96–104.

[41] Shaimardanova A. Alisa, Solovyeva V. Valeriya, Chulpanova S. Daria, James Victoria, Kitaeva V. Kristina, Rizvanov A. Albert, Extracellular vesicles in the diagnosis and treatment of central nervous system diseases, Neural Regen. Res. 15 (4) (2020) 586–596.

[42] Z. Wang, H. Liu, Lysine methylation regulates nervous system diseases, Neuropeptides 76 (2019), 101929.

[43] P. Monfort, C. Montoliu, C. Hermenegildo, Differential effects of acute and chronic hyperammonemia on signal transduction pathways associated to NMDA receptors, Neurochem. Int. 37 (2–3) (2000) 249–253.

[44] M. Shin, T.B. Ware, H.C. Lee, K.L. Hsu, Lipid-metabolizing serine hydrolases in the mammalian central nervous system: endocannabinoids and beyond, Biochim. Biophys. Acta 1864 (6) (2019) 907–921.

[45] H. Ma, S. Chen, H. Chen, L. Li, D. Li, J. Zhou, H. Pan, $\alpha 2\delta$-1 couples to NMDA receptors in the hypothalamus to sustain sympathetic vasomotor activity in hypertension, J. Physiol. 596 (17) (2018) 4269–4283.

[46] M. Hutterer, E. Bumes, M.J. Riemenschneider, AIDS-related central nervous system toxoplasmosis with increased 18F-fluoroethyl-L-Tyrosine amino acid PET uptake due to LAT1/2 expression of inflammatory cells, Clin. Nucl. Med. 42 (12) (2017) e506–e508.

[47] M. Farina, M. Aschner, Glutathione antioxidant system and methylmercury-induced neurotoxicity: an intriguing interplay, Biochim. Biophys. Acta 1863 (12) (2019), 129285.

[48] M. Bannai, K. Torii, Digestive physiology of the pig symposium: detection of dietary glutamate via gut-brain axis, J. Anim. Sci. 91 (5) (2013) 1974–1981.

[49] C.M. Kelsey, T. Grossmann, A call for mapping the development of the microbiota-gut-brain axis during human infancy, Behav. Brain Sci. 42 (2019) e74.

[50] J. Cases, V. Vacchina, A. Napolitano, B. Caporiccio, P. Besancon, R. Lobinski, J.M. Rouanet, Selenium from selenium-rich spirulina is less bioavailable than selenium from Sodium selenite and selenomethionine in selenium-deficient rats, J. Nutr. 131 (9) (2001) 2343–2350.

[51] H. Bozena, K. Marta, S. Sylvie, F. Carlos, R.N. Branislav, P. Qiuming, B. Mojmir, M. Magdalena, O. Radka, Z. Jarmila, B. Geir, S. Jiri, K. Rene, Nano-selenium and its nanomedicine applications: a critical review, Int. J. Nanomedicine 13 (2018) 2107–2128.